A novel multi-fiber Timoshenko beam finite element formulation with embedded discontinuities to describe reinforced concrete failure under static loadings

Ibrahim Bitar, Nathan Benkemoun, Panagiotis Kotronis, Stéphane Grange

A NOVEL MULTI-FIBER TIMOSHENKO BEAM FINITE ELEMENT FORMULATION WITH EMBEDDED DISCONTINUITIES TO DESCRIBE REINFORCED CONCRETE FAILURE UNDER STATIC LOADINGS

Ibrahim Bitar*, Nathan Benkemoun†, Panagiotis Kotronis* and Stéphane Grange‡

*École Centrale de Nantes, Université de Nantes, CNRS
Institut de Recherche en Génie Civil et Mcanique (GeM), UMR 6183
1 rue de la Noë, BP 92101, Nantes, cedex 3, France
e-mail: ibrahim.bitar@ec-nantes.fr ; panagiotis.kotronis@ec-nantes.fr

†IUT Saint-Nazaire, Université de Nantes, CNRS
Institut de Recherche en Génie Civil et Mcanique (GeM), UMR 6183
58 rue Michel Ange, 44600 Saint-Nazaire, France
e-mail: nathan.benkemoun@univ-nantes.fr

‡Université Grenoble Alpes, 3SR, F-38000 Grenoble, France
CNRS, 3SR, F38000 Grenoble, France
e-mail: stephane.grange@ujf-grenoble.fr

Key words: Timoshenko, Multi-fiber, Discontinuity

Abstract. A novel multi-fiber beam finite element formulation based on the Timoshenko model is proposed in this paper to simulate failure of reinforced concrete structural elements subjected to static monotonic loadings. The beam section can have an arbitrary shape and each fiber has a local constitutive law representing a specific material. The embedded discontinuity concept is adopted to enrich the displacement field of the fibers in order to describe the opening of cracks and the development of plastic hinges. The material behavior at the discontinuity is characterized by a cohesive law linking the axial stress and the displacement jump by a linear relation, which allows capturing the released fracture energy. The variational formulation is presented in the context of the incompatible modes method. Moreover, the additional modes are statically condensed at the element level. The corresponding computational procedure is detailed in the paper. Several numerical applications and general remarks are finally provided to illustrate the performance of the proposed element.

1 Introduction

Different kinematic assumptions are used in structural analysis in order to simplify the global equilibrium equations and to reduce the required number of degrees of freedom. The Timoshenko beam theory considers that plane sections remain plane after deformation but not necessary normal to the deformed axis. The advantage of this theory is that it takes into account the influence of shear strains (contrary to Euler-Bernoulli (EB) assumption.

In a multi-fiber beam context, the section of the beam is divided into several fibers with specific stress/strain relations [1]. Finite elements of this type are efficient for various applications in civil engineering: nonlinear analysis of beam type or bearing wall structures with non-homogenous sections (eg. reinforced concrete) [2], [3], arbitrarily geometrical plane or hollow shape sections [4], [5] submitted to bending,

shear or torsion [6], Soil Structure Interaction problems [4], vulnerability assessment cases [5] and Fiber-Reinforced Polymer retrofitting [7].

In this paper we present a novel multi-fiber beam finite element formulation based on the Timoshenko model to simulate failure of reinforced concrete structural elements subjected to static monotonic loadings. The new displacement-based Finite Element formulation proposed by [8] is used. This formulation uses shape functions of order three (3) for the transverse displacements, and two (2) for the rotations and an additional internal node. This results to a finite element free of shear locking. We refer to [9] where we show the performance of this formulation with respect to other formulations in the literature [10], [11].

The multi-fiber section consists of concrete and steel fibers. The concrete fibers behave according to a damage law and the steel fibers are modeled with an elasto-plastic behavior.

The lack of an internal length parameter in the behavior laws leads to mesh dependency. To solve this, different approaches can be found in the literature: local approaches [13], [14]; non local approaches [15], [16], [17]; and the enhanced approaches [18], [19]. In this work, the focus is set on the enhanced approach [19], and more specifically on the embedded discontinuity approach (EDA) [20]. EDA represents an alternative approach to the smeared and discrete crack representations avoiding some of their drawbacks as described in [21].

The EDA based on the strong discontinuity approach [19] is adopted, hence localized failure is incorporated into the standard disablement-based Finite Element using discontinuities variables. The fibers are enhanced in order to describe concrete crack openings and the development of plastic hinges for steel [22]. The strong discontinuity is introduced by adding a jump in the displacement field. Accordingly, additional shape functions are added to interpolate the displacement jump within the enhanced finite element.

Furthermore, the materials behavior at the discontinuity is characterized by a cohesive law linking the axial stress and the displacement jump by a linearly decreasing relation, which allows capturing the released fracture energy.

The variational formulation is presented in the context of the incompatible modes method. The additional modes are statically condensed at the element level in order to maintain the same architecture of the global resolution.

The outline of the paper is as follows. In the next section the governing equations of the multi-fiber Timoshenko beam with the corresponding interpolation functions describing the new based-displacement Finite Element [8] are briefly recalled. In section 3, we present shortly the behavior laws for continuum and cohesive materials. In section 4, we focus on the variational formulation. A numerical illustration of the proposed model is presented in section 5. The article ends with some concluding remarks.

2 Governing equations

Consider a beam of length Ł discretized into n elements $e = [x_i; x_j]$ of length $L = x_j - x_i$ and external nodes i and j. The generalized displacement vector is approximated by an equation of the form $U(x) = NU_e$, where U_e is a vector containing the external nodal displacements of the element e and N is the matrix of the shape functions depending on x. For simplicity reasons presentation is made hereafter in 2D.

$$U(x) = \begin{bmatrix} U_x(x) & U_y(x) & \Theta_z(x) \end{bmatrix}^T \quad (1)$$

$U_x(x)$ being the longitudinal displacement, $U_y(x)$ the transverse displacement and $\Theta_z(x)$ the rotation of the section at the neutral axis. The continuous displacements $\overline{u}_x(x, y), \overline{u}_y(x, y)$ of another point of the section (or of a "fiber" $f(x, y)$) can be evaluated using the displacements of the section as follows:

$$\begin{aligned} \overline{u}_x(x, y) &= U_x(x) - y\Theta_z(x), \\ \overline{u}_y(x, y) &= U_y(x) \end{aligned} \quad (2)$$

The strain field becomes:

$$\begin{aligned}\overline{\varepsilon}_x(x,y) =& \frac{\partial u_x}{\partial x} = U_x'(x) - y\Theta_z'(x),\\ \overline{\gamma}_{xy}(x,y) =& \frac{\partial u_x}{\partial y} + \frac{\partial u_y}{\partial x} = U_y'(x) - \Theta_z(x)\end{aligned} \tag{3}$$

with $\overline{\varepsilon}_x(x,y)$ the axial strain and $\overline{\gamma}_{xy}(x,y)$ the transverse shear strain of the fiber $f(x,y)$. The line over the variables indicates that they are continuous.

The theoretical formulation, based on equilibrium equations and the kinematic assumption and using the virtual work principle, provides the beam element stiffness matrix and the internal nodal forces expressions as follows

$$\begin{aligned}K_{element} &= \int_0^L B^T K_S B dx\\ F_{int,element} &= \int_0^L B^T F_S dx\end{aligned} \tag{4}$$

where B is a matrix containing the derivatives with respect to x of the shape functions, K_S is the multi-fiber section stiffness matrix and F_S is the generalized force vector of the section.

In order to enhance the element kinematics, the fiber axial displacement field (2) is written with an additional term ([23], [24], [25] and [22]), as follows:

$$u_x(x,y) = \overline{u}_x(x,y) + \alpha M_\alpha(x), \tag{5}$$

where $\overline{u}_x$ represents the continuum expression of the axial displacement (2) and

- $M_\alpha(x) = H_\alpha(x) - N(x),$ (6)
- $H_\alpha(x) = \{1 \text{ if } x > x_\alpha \text{ or } 0 \text{ if } x \leq x_\alpha\},$ (7)
- $N(x) = \dfrac{x}{L},$ (8)

and α is the discontinuity variable, x_α is the position of the discontinuity within the element. Therefore the enhanced axial strain field becomes:

$$\begin{aligned}\varepsilon_x(x,y) =& \frac{\partial}{\partial x}\left(\overline{u}_x(x,y)\right) + \frac{\partial}{\partial x}\left(\alpha M_\alpha(x)\right)\\ =& \overline{\varepsilon}_x(x,y) + \alpha\frac{\partial}{\partial x}\left(-N(x)\right) + \alpha\frac{\partial}{\partial x}\left(H_\alpha(x)\right)\\ =& \underbrace{\overline{\varepsilon}_x(x,y) + \alpha\ G(x)}_{\tilde{\varepsilon}} + \underbrace{\alpha\ \delta_\alpha(x)}_{\overline{\tilde{\varepsilon}}}\end{aligned} \tag{9}$$

where $\delta_\alpha(x)$ is the Dirac function at x_α. Thus, the latter expression of the axial strain is singular (presence of $\overline{\tilde{\varepsilon}}$). To solve this singularity, [26] proposed to introduce a cohesive law, that models the material discontinuity and thus eliminates the singular term.

2.1 Displacement-based Finite Element formulation

In this paragraph, the new displacement-based Full Cubic Quadratic Finite Element **FCQ** is presented [8]. Cubic functions are used to interpolate the transverse displacements and quadratic for the rotations. The element is free of shear locking and uses an additional internal node. Caillerie & al. [8] proved that one **FCQ** element is able to predict the exact tip displacements for any complex loading (shear/flexion) submitted to an homogeneous elastic beam (see also [9]).

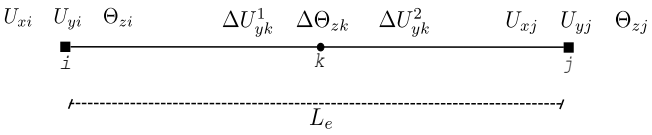

Figure 1: FCQ element

The nodal displacement field takes the following form, $U_e^T =$

$$[U_{xi}, U_{yi}, \Theta_{zi}, \Delta U^1_{yk}, \Delta\Theta_{zk}, \Delta U^2_{yk}, U_{xj}, U_{yj}, \Theta_{zj}],$$

where ΔU^1_{yk}, $\Delta\Theta_{zk}$ and ΔU^2_{yk} are the degrees of freedom of the internal node (with no specific physical meaning). The generalized displacement field is $U(x) = N(x)U_e$, and the interpolation functions matrix $N(x)$ can be found in the original paper [8] and also in the appendix.

3 Material Constitutive laws

The constitutive laws for the continuum and cohesive materials are briefly elaborated. We notice that shear components for both continuous models are linear elastic. Therefore the fiber shear stress is:

$$\tau = kG\gamma, \tag{10}$$

where k is the shear correction coefficient, G is the shear modulus and γ is the fiber elastic shear strain.

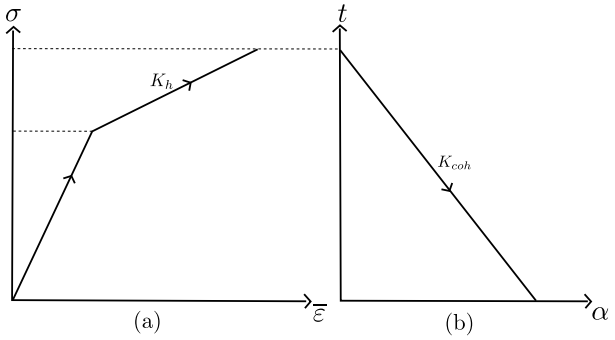

Figure 2: (a) Continuous model ; (b) Discontinuous model

3.1 Bulk concrete behavior

In order to model the concrete, a simple damage law based on the work of Ortiz 1985 [27] is used. The thermodynamic free energy for such model is expressed in function of the damage deformation $\overline{\varepsilon}^d$, the damage compliance modulus D and the strain-like hardening variable $\overline{\xi}^d$:

$$\overline{\Psi}^d = \overline{\sigma}^{dT}\overline{\varepsilon}^d - \frac{1}{2}\overline{\sigma}^{dT} D \overline{\sigma}^d + \frac{1}{2}\overline{\xi}^d K_h^d \overline{\xi}^d \quad (11)$$

The strain-strain relation can be deduced as:

$$\overline{\sigma}^d = D^{-1}\overline{\varepsilon}^d \text{ with } D \in [E_c^{-1}, \infty) \quad (12)$$

where E_c is the concrete young modulus. The hardening law takes a linear form $\overline{q}^d = K_h^d \overline{\xi}^d$ where K_h^d is the hardening modulus which is different in compression and traction. The damage criteria is defined by the following damage surface

$$\overline{\phi}^d = |\overline{\sigma}^d| - (\sigma_i^d - \overline{q}^d) \leq 0 \quad (13)$$

$$\sigma_i^d = \begin{cases} \sigma_c^d \text{ for compression} \\ \sigma_t^d \text{ for traction} \end{cases}$$

3.2 Bulk steel behavior

The steel fibers are modeled with an elasto-plastic behavior with isotropic hardening. The main ingredients of the model are given in the equations below. We start with the classical decomposition of the continuous strain into elastic and plastic terms:

$$\overline{\varepsilon} = \overline{\varepsilon}^e + \overline{\varepsilon}^p \quad (14)$$

The thermodynamic free energy is expressed in terms of the internal variables: the elastic deformation $\overline{\varepsilon}^e$ and the strain-like hardening variable $\overline{\xi}^s$.

$$\overline{\Psi}^s(\overline{\varepsilon}^e, \overline{\xi}^s) = \frac{1}{2}\overline{\varepsilon}^e E^s \overline{\varepsilon}^e + \frac{1}{2}\overline{\xi}^s K_h^s \overline{\xi}^s \quad (15)$$

where E^s is the steel elastic modulus and K_h^s is the steel hardening modulus. The stress/strain relation reads

$$\overline{\sigma}^s = E^s(\varepsilon - \overline{\varepsilon}^e) \text{ with } \begin{cases} \dot{\overline{\varepsilon}}^p = \dot{\gamma}\dfrac{\partial \overline{\phi}^s}{\partial \sigma} \\ \dot{\overline{\xi}}^s = \dot{\gamma}\dfrac{\partial \overline{\phi}^s}{\partial q} \end{cases} \quad (16)$$

where $\overline{q}^s$ is the stress-like variable defining the linear hardening law $\overline{q}^s = K_h^s \overline{\xi}$ and $\overline{\phi}^s$ is the elastic yield surface:

$$\overline{\phi}^s = |\overline{\sigma}^s| - (\overline{\sigma}_e^s - \overline{q}^s) \leq 0. \quad (17)$$

3.3 Cohesive material behavior at the discontinuity

Linear cohesive laws are used. The thermodynamic free energies relative to concrete and steel:

$$\overline{\overline{\Psi}}^d = \tfrac{1}{2} K_{coh}^{d^2} \overline{\overline{\xi}}^d \quad , \quad \overline{\overline{\Psi}}^s = \tfrac{1}{2} K_{coh}^{s^2} \overline{\overline{\xi}}^s \quad (18)$$

K_{coh} is the softening modulus (< 0) of the cohesive material. The cohesive laws are expressed as a relation between the traction at the discontinuity and the discontinuity variable:

$$t^d = K_{coh}^d \alpha^d \quad , \quad t^s = K_{coh}^s \alpha^s \quad (19)$$

In order to pass from the continuum model to the discrete one, a failure criteria should be verified. This criteria is defined by the function $\overline{\overline{\phi}}$ such that:

$$\overline{\overline{\phi}}^i = |t(\alpha^i)| - (\sigma_u^i - \overline{\overline{q}}^i) \leq 0 \quad (20)$$

where $\overline{\overline{q}}^i = -\dfrac{\partial \overline{\overline{\Psi}}^i}{\partial \overline{\overline{\xi}}^i} = -K_{coh}^i \overline{\overline{\xi}}^i$ and $i = \{d, s\}$.

4 Variational formulation

The objective of this work is to embed discontinuity into the fiber axial displacement field. In the spirit of the Hu-Washizu variational formulation [28], [29], the variational formulation can be written within the framework of a finite element problem and leads to the following set of non linear equations,

$$\bigwedge_{e=1}^{n_{elem}} \bigwedge_{f=1}^{n_{fib}^{act}} \left[f_{e,f}^{int}(U_e, \alpha_{e,f}) - f_{e,f}^{ext} \right] = 0 \tag{21}$$

$$h_{e,f}(U_e, \alpha_{e,f}) = 0, \forall e \in [1, n_{elm}], \forall f \in [1, n_{fib}^{act}] \tag{22}$$

where $\bigwedge$ denotes the standard assembly operator, n_{fib}^{act} indicates the fibers with active discontinuity. The first equation above concerns the global equilibrium, and the second one is relative to the local equilibrium corresponding to the active embedded discontinuities in the fibers (n_{fib}^{act}).

The linearized form of the system of equations (21) at incremental pseudo-time $n+1$ and iteration $k+1$ reads

$$\bigwedge_{e=1}^{n_{elem}} \bigwedge_{f=1}^{n_{fib}^{act}} \left\{ \begin{bmatrix} K_{BB} & K_{BG} \\ K_{GB} & K_{GG} + K_{coh} \end{bmatrix}_{n+1}^{k} \begin{bmatrix} \Delta U_{e,f} \\ \Delta \alpha_{e,f} \end{bmatrix}_{n+1}^{k+1} = \begin{bmatrix} f_{e,f}^{int} - f_{e,f}^{ext} \\ h_{e,f} \end{bmatrix}_{n+1}^{k} \right\} \tag{23}$$

where,

$$K_{BB} = \frac{\partial f_{e,f}^{int}}{\partial U_{e,f}} = \int_{V_f} B_f^T K_f B_f dV_f; \tag{24}$$

$$K_{BG} = \frac{\partial f_{e,f}^{int}}{\partial \alpha_{e,f}} = \int_{V_f} B_f^T K_f G_f dV_f; \tag{25}$$

$$K_{GB} = \frac{\partial h_{e,f}}{\partial U_{e,f}} = \int_{V_f} G_f^T K_f B_f dV_f; \tag{26}$$

$$K_{GG} = \frac{\partial h_{e,f}}{\partial \alpha_{e,f}} = \int_{V_f} G_f^T K_f G_f dV_f; \tag{27}$$

and B^f represents the interpolation function of the strain field at the fiber level, G^f is the enhanced interpolation function, $U_{e,f}$ is the nodal displacements of the fiber and K_f is the material tangent modulus of the fiber.

The local equilibrium equation represented by the second equation of the linearized system (23) is solved locally for the active discontinuities, therefore, we find the increment of the jump $\Delta\alpha_{e,f}$. Using the static condensation technique, the following condensed fiber stiffness is found

$$K_{cond} = K_{BB} - K_{BG} K_{GG}^{-1} K_{GB} \tag{28}$$

5 Numerical applications

To illustrate our model, two numerical applications are presented hereafter.

5.1 Application 1

In order to prove the efficiency of the enhancement method to solve the mesh dependence problem, we consider a cantilever beam of length Ł $= 1m$ subjected to transverse displacement at the right end. Firstly, the fibers of the beam are modeled with an elasto-plastic material with continuum softening. The beam is tested with several mesh sizes. Secondly, the fibers are modeled with an elasto plastic behavior for the continuum part coupled to a cohesive law for the softening part. The results of both applications are showed in the figures below.

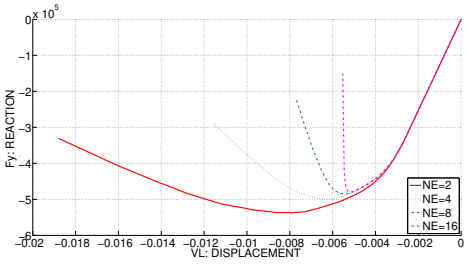

Figure 3: Elasto-plastic model with continuous softening

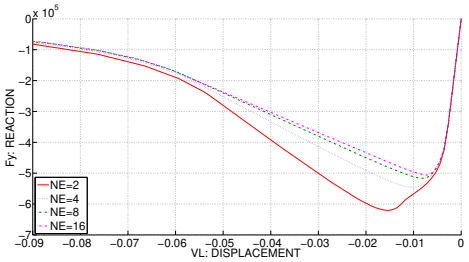

Figure 4: Elasto-plastic model with cohesive law

The difference between the figures (3) and (4) is clear. The elasto-plastic behavior with continuum softening is not objective relative to the mesh size as we can see in figure (3). Indeed, the quantity of dissipated energy decreases with fine discretization. On the other hand, the enhanced multi-fiber beam improved the softening response with respect to mesh dependency since all the curves in figure (4) coincide at the end of the softening phase. Nevertheless, the total response is not yet free of mesh dependence. Furthermore, the dissipated energy in the beam softening response for the enhanced beam is captured by the cohesive law according to the following expression $\overline{\overline{D}} = t\dot{\alpha} - \dot{\overline{\overline{\Psi}}}$; therefore, since discontinuities appear only in the first element whatever the mesh size, the captured energy in the softening process is the same.

The strain localization is also examined at local level. The axial strain distribution in the extreme fiber (located at section's edge) along the beam length is showed with both models (with and without enhancement) in figures (5), (6). The curves are obtained by joining the strain values at the integration points of the elements. We remark that the strain localization is regularized once the fiber is enhanced. Figure (5) clearly shows the strain localization within the first element of the fiber by refining the mesh of the beam. Otherwise, one can notice the presence of active discontinuity in the first enhanced element of the fiber by the decreased strain values within the element, (6).

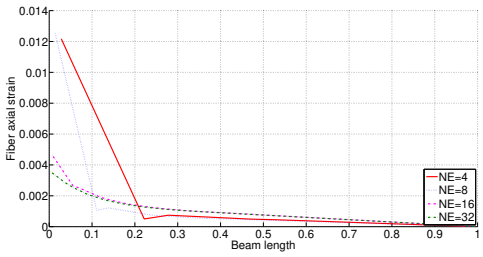

Figure 5: Strain at fiber level : Elasto-plastic model with continuous softening

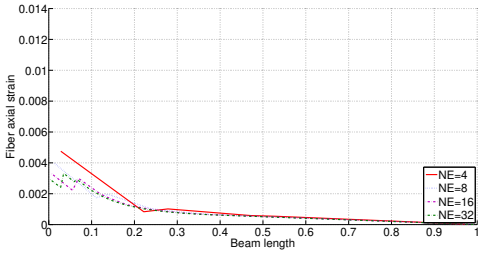

Figure 6: Strain at fiber level : Elasto-plastic model with cohesive law

Furthermore, figure (7) shows that the number of the fibers in the section doesn't have a big influence on the global response of the beam discretized into two elements.

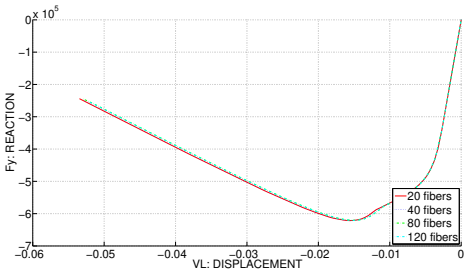

Figure 7: Influence of the fibers number on the global response

5.2 Application 2

We consider a cantilever reinforced concrete beam with fixed support at the left end, and submitted to transversal displacement at the free end. The beam has a length of Ł $= 1m$ and the section (0.2×0.5) is divided into 62 fibers (figure (8)). 2 bars of diameter $32mm$ are added to the top of the section as reinforcement (fiber 4 in figure (8)). The materials properties are the following:

Concrete properties

$$E_c = 40 \text{ GPa} \qquad K^d_{coh} = -5.2 \text{ GPa}$$
$$\nu_c = 0.2 \qquad \sigma^{comp}_{elastic} = 40 \text{ MPa}$$
$$K^d_h = 2 \text{ GPa} \qquad \sigma^{comp}_{crack} = 45 \text{ MPa}$$
$$\sigma^{trac}_{crack} = 7 \text{ MPa}$$

Steel properties

$E_s = 200$ GPa $\quad K^s_{coh} = -0.5$ GPa
$\nu_s = 0.3$ $\quad \sigma^s_{elastic} = 80$ MPa
$K^s_h = 30$ GPa $\quad \sigma^s_{ultimate} = 90$ MPa

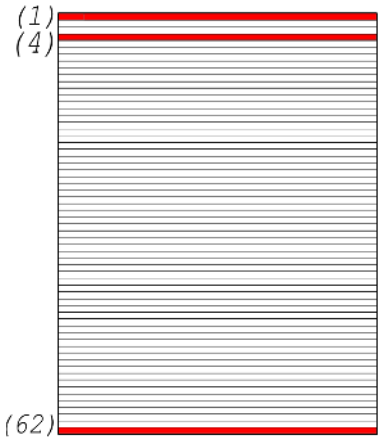

Figure 8: Multi-fiber section

The global response of the reinforced beam, the cohesive law at an active discontinuity and the behavior of the extreme compressed fiber are showed in the figures below:

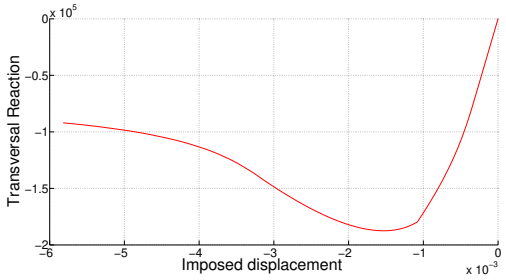

Figure 9: Global response of the enhanced multi-fiber reinforced concrete beam

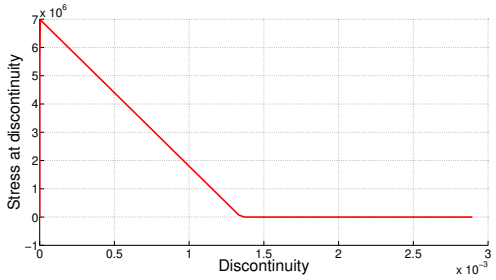

Figure 10: Cohesive law at the active discontinuity within extreme concrete fiber (1)

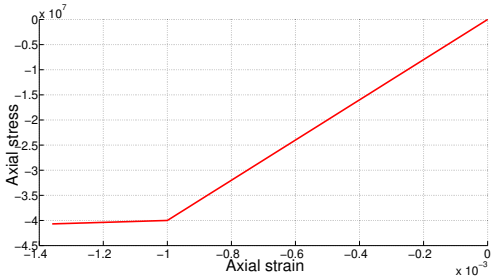

Figure 11: Behavior of the extreme compressed concrete fiber (62)

Figure (11) shows that the extreme compressed concrete fiber (number (62) in fig. (8)) is in the hardening phase. Figure (10) shows that the extreme tight concrete fiber (1) is totally cracked.

6 Conclusion

In this paper, a new multi-fiber displacement based Timoshenko Finite Element is proposed. Higher order shape functions with additional internal degrees of freedom are used to interpolate the element displacement field. The embedded discontinuity approach is used to enhance the kinematic of the fibers. Therefore, the objectiveness of the softening response with respect to the mesh size is improved. The section is divided into fibers of concrete and steel. Each material is modeled with two coupled behaviors, a continuous model to describe the bulk behavior and a cohesive model to illustrate the localized zones. The variational formulation is briefly elaborated. A numerical illustration of the proposed model is presented and it showed that the strain localization is limited. We are currently working on improving the discontinuity kinematic of the enhanced fibers, and we look to extend the current model to make cyclic applications in the forthcoming work.

Acknowledgments

The authors would like to thank the PIA-SINAPS@ project (Sésisme et Installation Nucléaire: Améliorer et Pérenniser la Sureté), approved and funded by the National Agency of Research (ANR) following the RSNR 2012 call for projects on future investments post-

Fukoshima. (SINAPS@ ANR-11-RSNR-0022)

REFERENCES

[1] D. R. Owen, E. Hinton, Finite elements in plasticity, Pineridge press, 1980.

[2] P. Kotronis, F. Ragueneau, J. Mazars, A simplified modelling strategy for R/C walls satisfying PS92 and EC8 design, Engineering Structures 27 (8) (2005) 1197–1208.

[3] S. Grange, P. Kotronis, J. Mazars, Numerical modelling of the seismic behaviour of a 7-story building: NEES benchmark, Materials and Structures 42 (10) (2008) 1433–1442.

[4] S. Grange, L. Botrugno, P. Kotronis, C. Tamagnini, The effects of Soil-Structure Interaction on a reinforced concrete viaduct, Earthquake Engineering & Structural Dynamics 41 (11) (2011) 1549–1568.

[5] C. Desprez, P. Kotronis, J. Mazars, Seismic vulnerability assessment of a RC structure before and after FRP retrofitting, Bulletin of Earthquake Engineering 13 (2015) 539–564.

[6] J. Mazars, P. Kotronis, F. Ragueneau, G. Casaux, Using multifiber beams to account for shear and torsion, Computer Methods in Applied Mechanics and Engineering 195 (52) (2006) 7264–7281.

[7] C. Desprez, J. Mazars, P. Kotronis, P. Paultre, Damage model for FRP-confined concrete columns under cyclic loading, Engineering Structures 48 (2013) 519–531.

[8] D. Caillerie, P. Kotronis, R. Cybulski, A Timoshenko finite element straight beam with internam degrees of freedom, International Journal for Numerical and Analytical Methods in Geomechanics 39 (16) (2015) 1753–1773.

[9] I. Bitar, S. Grange, P. Kotronis, N. Benkemoun, A review on Timoshenko multifiber beams Finite Element formulations and elasto-plastic applications (under review), European Journal of Environnemental and Civil Engineering.

[10] P. Pegon, A Timoshenko simple beam element in Castem 2000.

[11] J. Guedes, P. Pegon, A. V. Pinto, A Fibre/Timoshenko beam element in Castem 2000.

[12] F. Armero, D. Ehrlich, An analysis of strain localization and wave propagation in plastic models of beams at failure, Computer Methods in Applied Mechanics and Engineering 193 (30-32) (2004) 3129–3171.

[13] A. Hillerborg, Application of fracture mechanics to concrete: summary of a series of lectures 1988, Div of Building Materials LTH, Lund university, 1988.

[14] A. Needleman, Material rate dependence and mesh sensitivity in localization problems, Computer Methods in Applied Mechanics and Engineering 67 (1) (1988) 69–85.

[15] Z. P. Bažant, T. B. Belytschko, Wave propagation in a strain-softening bar: exact solution, Journal of Engineering Mechanics 111 (3) (1985) 381–389.

[16] Z. P. Bažant, J. Pan, G. Pijaudier?Cabot, Softening in Reinforced Concrete Beams and Frames, Journal of Structural Engineering 113 (12) (1987) 2333–2347.

[17] R. Chambon, D. Caillerie, N. El Hassan, Etude de la localisation unidimensionnelle à l'aide d'un modèle de second gradient, Comptes rendus de l'Académie des sciences. Série II, Mécanique, physique, chimie, astronomie 323 (4) (1996) 231–238.

[18] M. Ortiz, Y. Leroy, A. Needleman, A finite element method for localized failure analysis, Computer Methods in Applied Mechanics and Engineering 61 (2) (1987) 189–214.

[19] J. C. Simo, J. Oliver, F. Armero, An analysis of strong discontinuities induced by strain-softening in rate-independent inelastic solids, Computational Mechanics 12 (5) (1993) 277–296.

[20] G. Wells, L. Sluys, Application of embedded discontinuities for softening solids, Engineering Fracture Mechanics 65 (2-3) (2000) 263–281.

[21] H. R. Loffi, P. B. Shing ', Embedded Representation of Fracture in Concrete With Mixed Finite Elements, International Journal for Numerical Methods in Engineering 38 (July 1994) (1995) 1307–1325.

[22] M. Jukić, B. Brank, A. Ibrahimbegović, Failure analysis of reinforced concrete frames by beam finite element that combines damage, plasticity and embedded discontinuity, Engineering Structures 75 (2014) 507–527.

[23] F. Armero, On the characterization of localized solutions in inelastic solids: an analysis of wave propagation in a softening bar, Computer Methods in Applied Mechanics and Engineering 191 (3-5) (2001) 181–213.

[24] D. Ehrlich, F. Armero, Finite element methods for the analysis of softening plastic hinges in beams and frames, Computational Mechanics 35 (4) (2005) 237–264.

[25] B. H. Pham, D. Brancherie, L. Davenne, A. Ibrahimbegović, Stress-resultant models for ultimate load design of reinforced concrete frames and multi-scale parameter estimates, Computational Mechanics 51 (3) (2013) 347–360.

[26] A. Ibrahimbegović, D. Brancherie, Combined hardening and softening constitutive model of plasticity: Precursor to shear slip line failure, Computational Mechanics 31 (1-2 SPEC.) (2003) 88–100.

[27] M. Ortiz, A constitutive theory for the inelastic behavior of concrete 4 (1985) 67–93.

[28] K. Washizu, Variational methods in elasticity and plasticity, Vol. 9, 1984.

[29] T. B. Belytschko, J. Fish, B. E. Engelmann, A finite element with embedded localization zones* 70 (1988) 59–89.

Appendix A FCQ element

The interpolation functions of the new displacement based Full Cubic Quadratic Finite Element FCQ [8] are

$$N(x) = \begin{bmatrix} N_1 & 0 & 0 & 0 & 0 & 0 & N_7 & 0 & 0 \\ 0 & N_{11} & 0 & N_{13} & 0 & N_{15} & 0 & N_{17} & 0 \\ 0 & 0 & N_{21} & 0 & N_{23} & 0 & 0 & 0 & N_{27} \end{bmatrix} \tag{29}$$

$$\text{where} \begin{cases} N_1 = 1 - \frac{x}{L} \\ N_7 = \frac{x}{L} \\ N_{11} = (1 - \frac{x}{L})^2(1 + 2\frac{x}{L}) \\ N_{13} = 2(1 - \frac{x}{L})^2(\frac{x}{L}) \\ N_{15} = -2(\frac{x}{L})^2(1 - \frac{x}{L}) \\ N_{17} = (\frac{x}{L})^2(3 - 2\frac{x}{L}) \\ N_{21} = (1 - \frac{x}{L})(1 - 3\frac{x}{L}) \\ N_{23} = 1 - (1 - 2\frac{x}{L})^2 \\ N_{27} = -(\frac{x}{L})(2 - 3\frac{x}{L}) \end{cases} \tag{30}$$

The three internal degrees of freedom can be treated locally (inside the element subroutine) using static condensation method (see [8] for more details and the analytical expressions of the condensed matrices and vectors).